Electronic Supplementary Information

Hybrid films with excellent oxygen and water vapor barrier properties as efficient anticorrosive coatings

Jiajie Wang, Ting Pan, Jian Zhang, Xiaozhi Xu, Qing Yin, Jingbin Han* and Min Wei

State Key Laboratory of Chemical Resource Engineering, Beijing Advanced Innovation Center for Soft Matter Science and Engineering, Beijing University of Chemical Technology, Beijing 100029, P. R. China.

Author Information

∗ Corresponding author. Phone: +86-10-64412131. Fax: +86-10-64425385.

E-mail: hanjb@mail.buct.edu.cn

Characterization techniques. X-ray diffraction (XRD) patterns were recorded by a Rigaku XRD-6000 diffractometer, using Cu Kα radiation (λ = 0.1542 nm) at 40 kV, 30 mA. Fourier transform infrared (FT-IR) spectra were obtained using a Nicolet IS50 (Thermo) spectrophotometer with 2 cm^{-1} resolution. The particle size distribution was carried out using a Malvern Mastersizer 2000 laser particle size analyzer. UV-vis absorption and transmittance spectra were collected on a Shimadzu U-3000 spectrophotometer. Thermogravimetric analysis (TGA) was performed on HCT-1 thermal gravimetric analyzer (Beijing Henven Scientific Instument Factory) with the temperature range from 20℃ to 700℃ at a heating rate of 10℃/min. The morphology was investigated using a scanning electron microscope (SEM; Zeiss SUPRA 55) with the accelerating voltage of 20 kV. The $(LDH\text{-}80/PDMS)_n$ films on quartz glass substrate were engraved a trace on the opposite side and steeped into liquid nitrogen for 1 min, followed by a careful cutting. The thickness of the films was obtained from the crack area by side-view SEM observation. The surface roughness data were obtained by using a NanoScope IIIa atomic force microscope (AFM) from Veeco Instruments. The oxygen transmission rate (OTR) was measured using a VAC-V2 gas transmission rate testing equipment. The water vapor transmission rate (WVTR) was collected using a W3/060 testing system. All the permeability coefficient values were averaged from at least five separate films. The grazing incidence X-ray diffraction (GIXRD) measurements were carried out in the Shanghai Synchrotron Radiation Facility (SSRF), executed by a X-ray with incident angle of 0.15° and exposure time of 60 s. Two-dimensional (2D) GIXRD patterns were obtained by a Mar CCD mounted vertically with a distance of ~178 mm to the sample. A FEI Cs-corrected Titan 80-300 high resolution transmission electron microscope (HRTEM) was operated at 300 kV to detect the orientation of LDH platelets in the hybrid films. The $(LDH\text{-}80/PDMS)_n$ film was embedded into 812 epoxy resin, refrigerated in liquid nitrogen and finally cut into ultrathin slices to obtain the samples for TEM observation.

Supplementary Figures

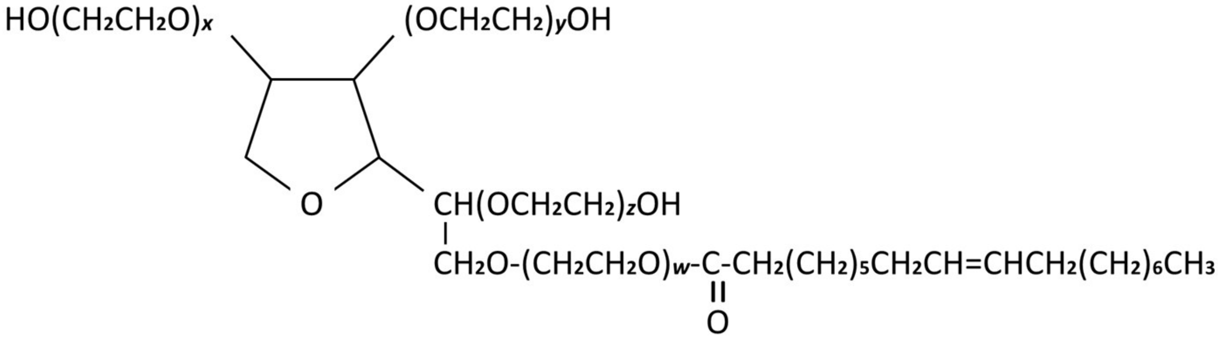

Fig. S1 Chemical structural formula of Tween 80 (w+x+y+z = 20).

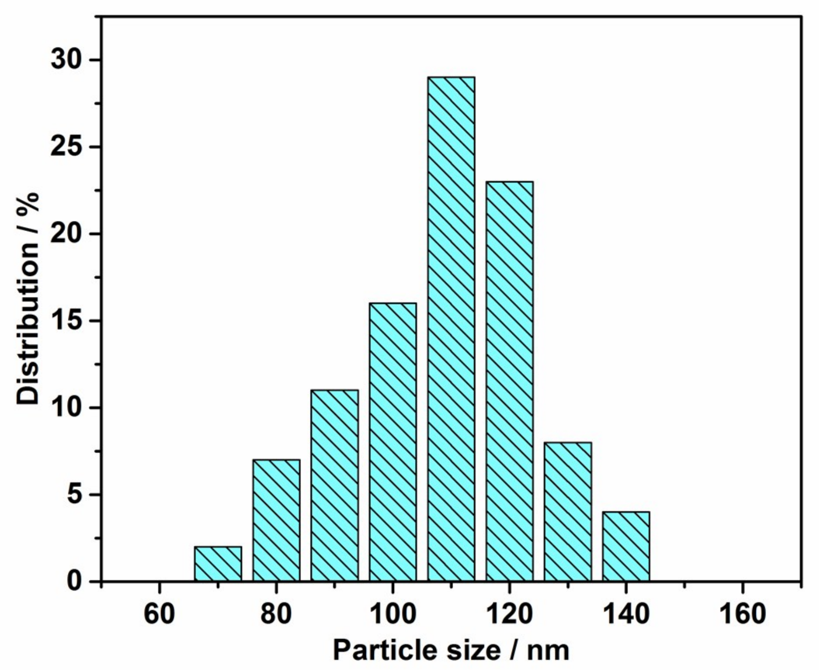

Fig. S2 Particle size distribution of LDH-80 nanoplatelets.

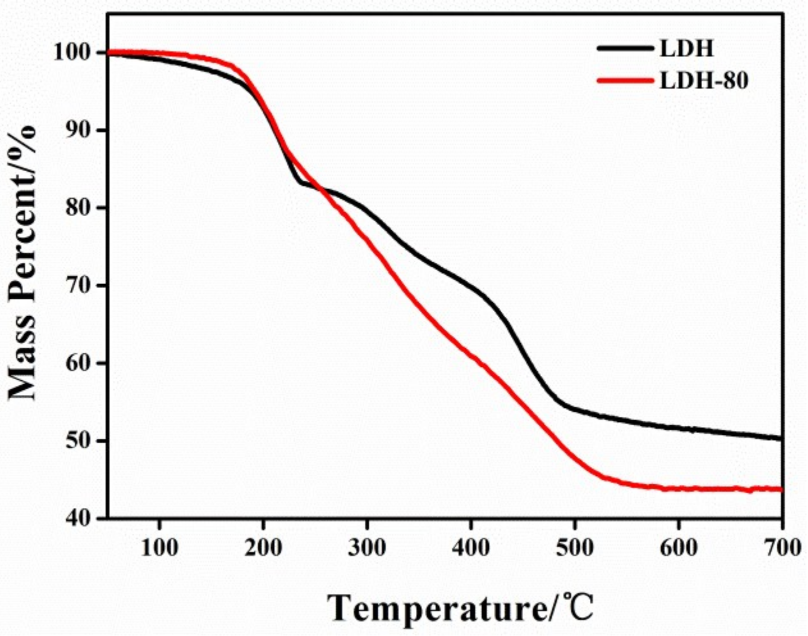

Fig. S3 Thermogravimetric analysis (TGA) of LDH and LDH-80.

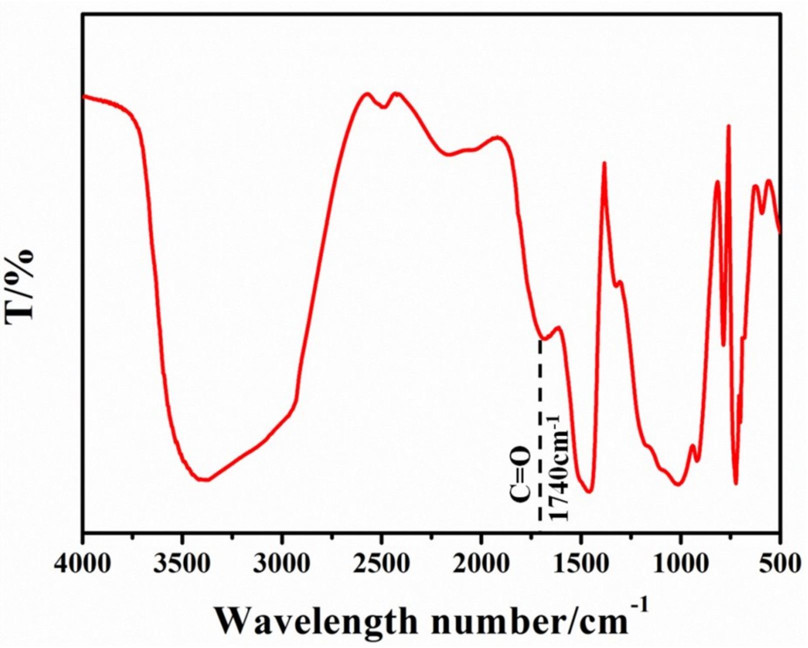

Fig. S4 FT-IR spectrum for physical mixture of LDH and Tween 80.

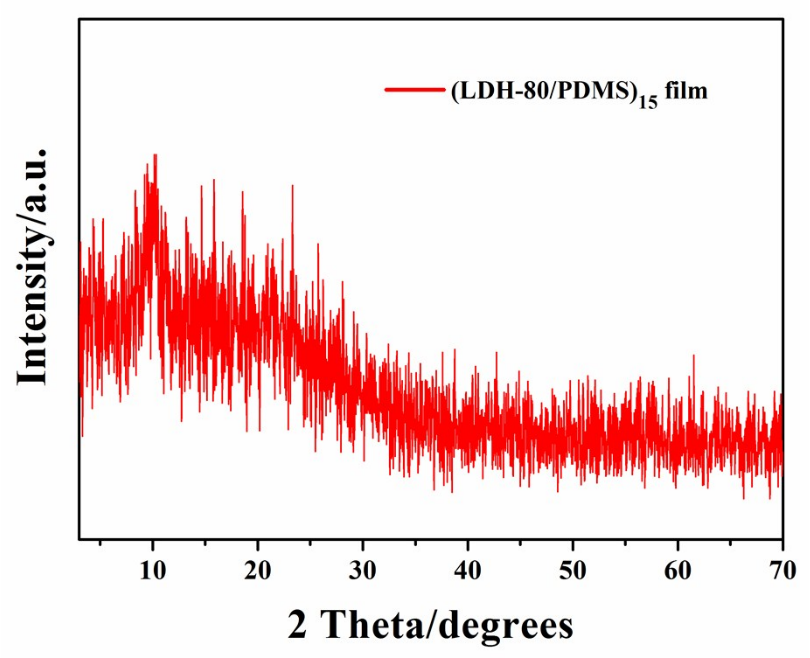

Fig. S5 XRD pattern of the (LDH-80/PDMS)$_{15}$ film.

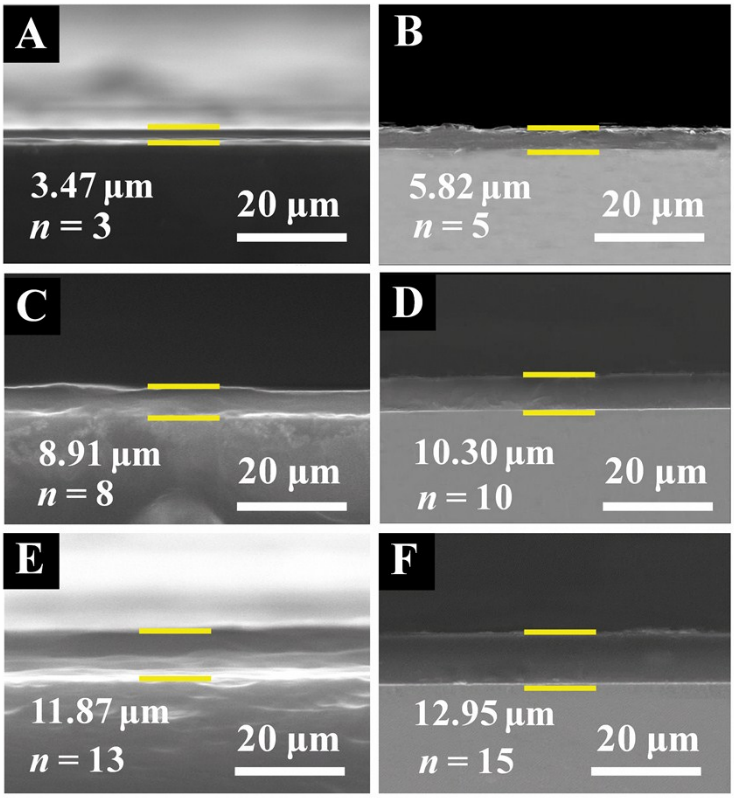

Fig. S6 Side-view SEM images of (LDH-80/PDMS)$_n$ (n = 3−15) films (the image F is reproduced from the inset of Fig. 3B, for ease of comparison).

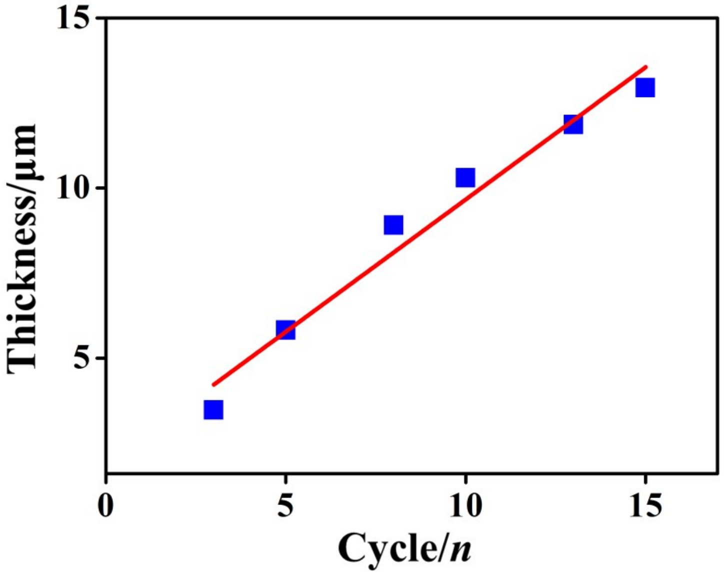

Fig. S7 The linear relationship between the thickness and bilayer number (*n*) of $(LDH\text{-}80/PDMS)_n$ (n = 3−15) films.

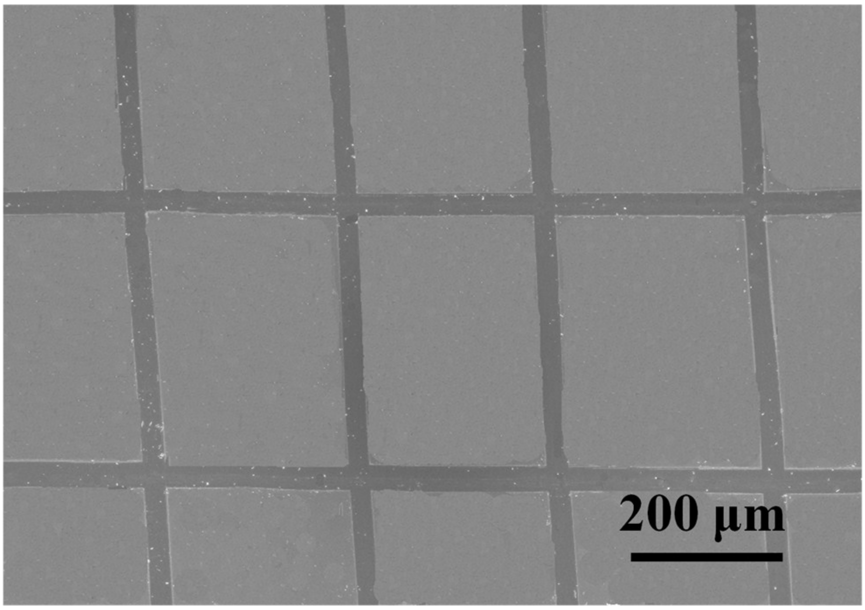

Fig. S8 SEM image of the $(LDH\text{-}80/PDMS)_{15}$ film on PET substrate after scratching on its surface.

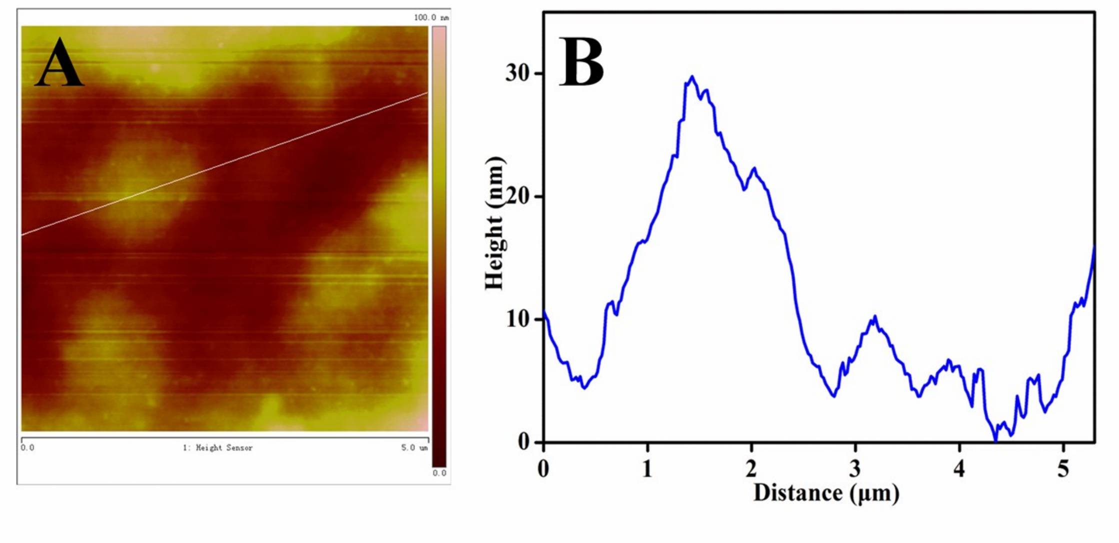

Fig. S9 (A) AFM topographical image (5 μm × 5 μm) of $(LDH\text{-}80/PDMS)_{15}$ film and (B) respective surface profile along the marked white line in the topographical image.

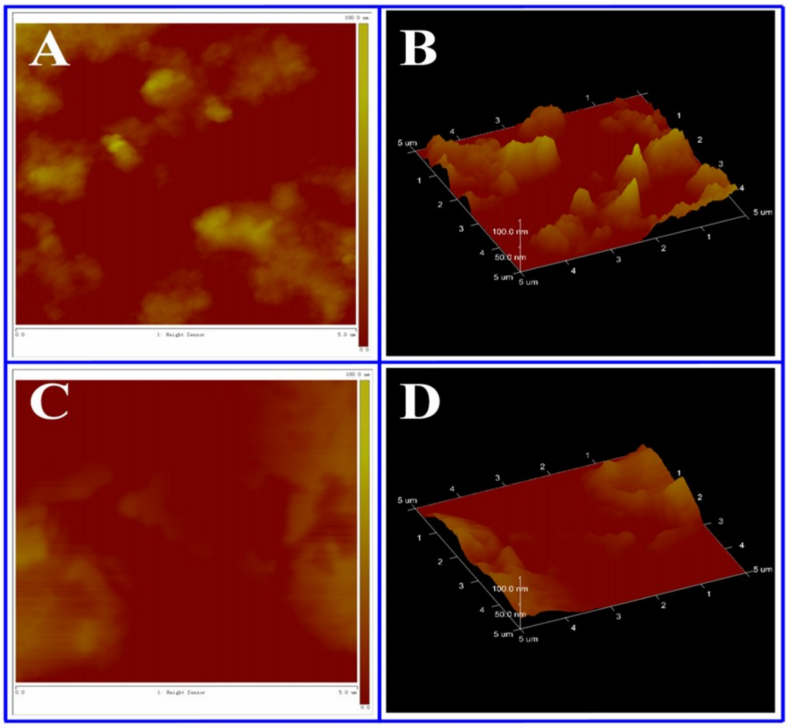

Fig. S10 AFM topographical images (5 μm × 5 μm) of (A, B) $(LDH/PDMS)_{15}$ and (C, D) pure PDMS film.

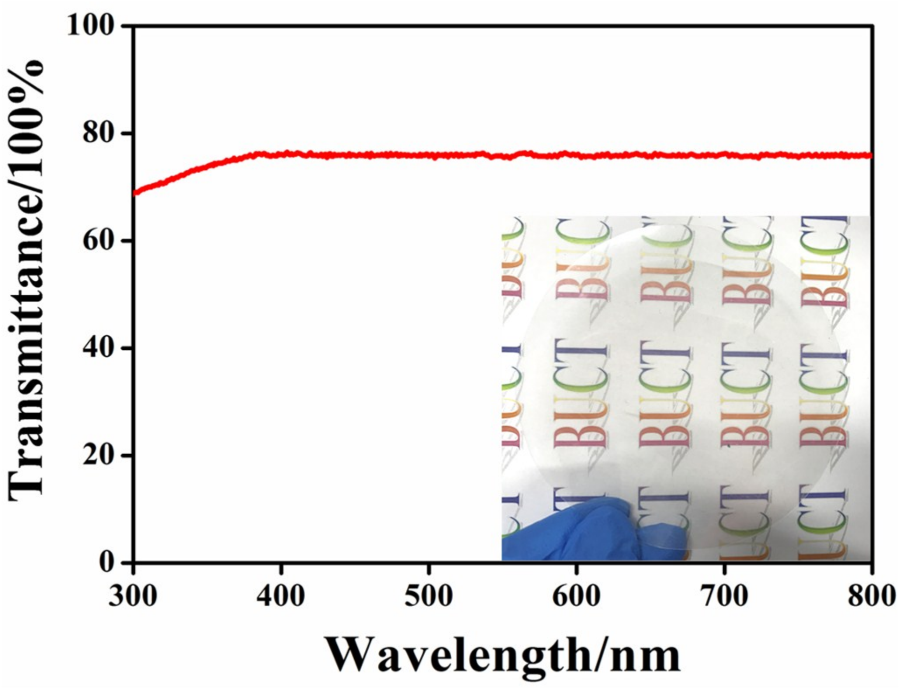

Fig. S11 The UV-vis transmittance spectrum (inset: photograph) of the (LDH/PDMS)$_{15}$ film.

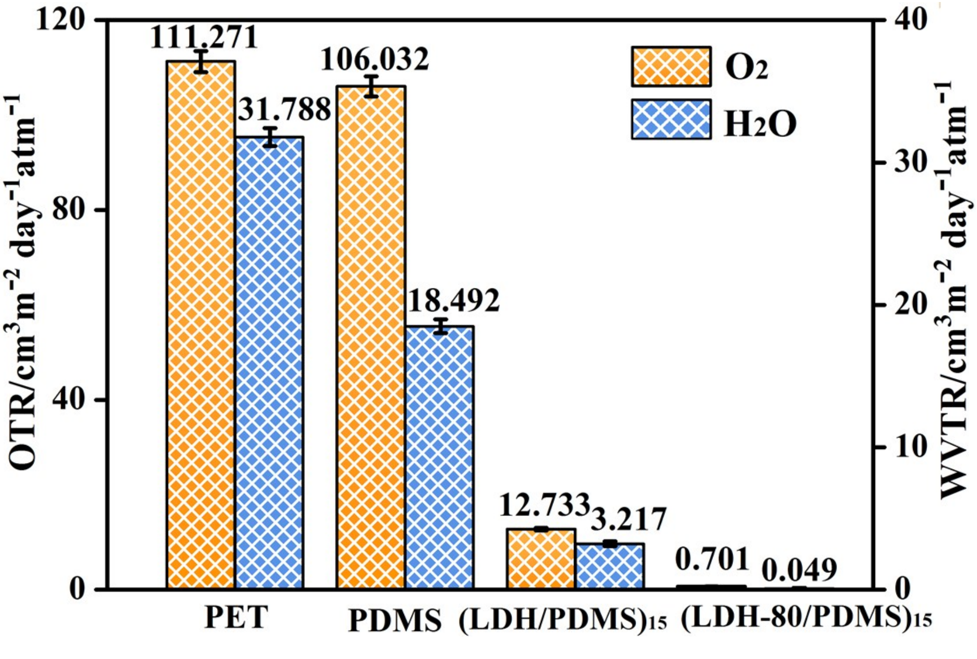

Fig. S12 OTR and WVTR values of PET substrate, PDMS (with the same thickness as (LDH-80/PDMS)$_{15}$ film), (LDH/PDMS)$_{15}$ and (LDH-80/PDMS)$_{15}$ film on PET substrate, respectively.

Table S1. Comparison between (LDH-80/PDMS)$_n$ film and other reported materials in oxygen and water vapor barrier properties.

Film material	**WVTR**	**OTR**	**Thickness of coating**	**Ref.**
PI/Alns	8.5	\	702 nm (on PET substrate)	1
Polyimide/TRG	2.0	\	8.1 μm (free standing)	2
PU/OM	24.5	\	606 nm (on PP substrate)	3
Nylon/FG	4.6	\	12.6 μm (on PET substrate)	4
COC/TRGO	0.7	\	270 nm (free standing)	5
EVOH/exfoliated graphite	1.29	\	863 nm (on PP substrate)	6
F-HG BPSQ	20.3	\	469 nm (on PET substrate)	7
Surlyn/magnesium oxide	0.07	\	16.3 μm (free standing)	8
Spider silk protein/nanoclay	0.2	2.3	12.5 μm (on copy-paper substrate)	9
$(PEI/PAA)_{50}$	0.8	\	19.5 μm (free standing)	10
$(PEI/MMT)_{20}$	\	3.0	9.2 μm (on PS substrate)	11
$(PVP/MMT)_{40}$	\	3.9	7.1 μm (on PET substrate)	12
Epoxy/Na^+-MMT	\	1.0	10.6 μm (on PET substrate)	13
Pullulan/clay	\	1.4	13.4 μm (on PP substrate)	14
$(U\text{-}mLDH/NBR)_{20}$	\	2.8	1.04 μm (on PET substrate)	15
$(CS_{pH4}/CNs_{pH2})_{15}$	\	1.3	15.2 μm (free standing)	16
$(Graphene/poly\text{-}electrolyte)_{20}$	\	0.9	310 nm (free standing)	17
$(LDH\text{-}80/PDMS)_{15}$	~ 0.05	~ 0.7	12.95 μm (on PP substrate)	This work

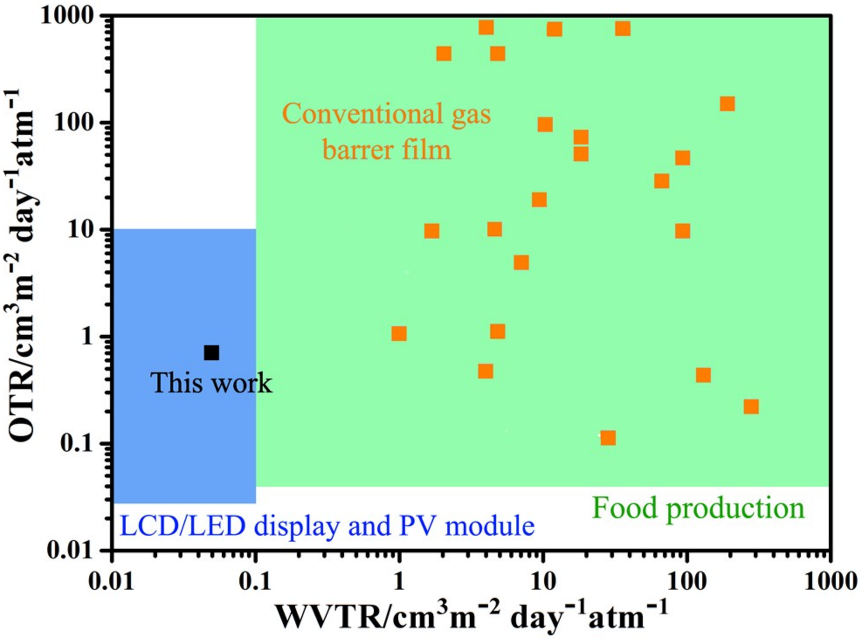

Fig. S13 Comparison between (LDH-80/PDMS)$_n$ and conventional polymer films used for oxygen/water vapor barrier applications.[18,19]

References

[1] I. Tseng, M. Tsai and C. Chung, *ACS Appl. Mater. Interfaces*, 2014, **6**, 13098−13105.

[2] M. Tsai, I. Tseng, Y. Liao and J. Chiang, *Polym Int*, 2013, **62**, 1302−1309.

[3] M. Osman, V. Mittal, M. Morbidelli and U. Suter, *Macromolecules,* 2003, **36**, 9851−9858.

[4] J. Jin, R. Rafiq, Y. Q. Gill and M. Song, *Eur Polym J*, 2013, **49**, 2617−2626.

[5] C. Lai, Y. Fu, J. Chen, D. Wang, Y. Sun, S. Huang, W. Hung, C. Hu and K. Lee, *Carbon*, 2015, **90**, 85−93.

[6] H. Kwon, D. Kim, J. Seo and H. Han, *Macromol. Res.,* 2013, **21**, 987−994.

[7] C. Zhang, C. Zhang, R. Ding, X. Cui, J. Wang, Q. Zhang and Y. Xu, *ACS Appl. Mater. Interfaces*, 2016, **8**, 14766−14775.

[8] S. Gupta, S. Seethamraju, P. C. Ramamurthy and G. Madras, *Ind. Eng. Chem. Res.*, 2013, **52**, 4383−4394.

[9] D. Zhang and H. Xiao, *ACS Appl. Mater. Interfaces*, 2013, **5**, 3464−3468.

[10] Y. Yang, L. Bolling, M. Haile and J. C. Grunlan, *RSC Adv.,* 2012, **2**, 12355−12363.

[11] M. A. Priolo, D. Gamboa and J. C. Grunlan, *ACS Appl. Mater. Interfaces*, 2010, **2**, 312−320.

[12] K. M. Holder, M. A. Priolo, K. E. Secrist, S. M. Greenlee, A. J. Nolte and J. C. Grunlan, *J. Phys. Chem. C*, 2012, **116**, 19851−19856.

[13] K. S. Triantafyllidis, P. C. LeBaron, I. Park and T. J. Pinnavaia, *Chem. Mater*., 2006, **18**, 4393−4398.

[14] L. Introzzi, T. Blomfeldt, S. Trabattoni, S. Tavazzi, N. Santo, A. Schiraldi, L. Piergiovanni and S. Farris, *Langmuir*, 2012, **28**, 11206−11214.

[15] L. Wang, Y. Dou, J. Wang, J. Han, L. Liu and M. Wei, *Composites: Part A*, 2017, **102**,

314−321.

[16] F. Li, P. Biagioni, M. Finazzi, S. Tavazzi and L. Piergiovanni, *Carbohydrate Polymers*, 2013, **92**, 2128−2134.

[17] A. A. Gokhale, J. Lu, N. J. Parker, A. P. Izbicki, O. Sanyal and I. Lee, *Journal of Colloid and Interface Science*, 2013, **409,** 219−226.

[18] B. M. Yoo, H. J. Shin, H. W. Yoon and H. B. Park, *J. Appl. Polym. Sci.*, 2014, 2013, **131**, 1−15.

[19] J. Lange and Y. Wyser, *Packaging Technol. Sci.*, 2003, **16**, 149−158.